engineering proceedings

MDPI

Proceeding Paper

Electrodeposition of Nickel-Based Thin Layered Double Hydroxides Electrocatalyst for 2,5-Diformylfuran Production †

Nadia Mumtazah [1], Nurfadlih Syahlani [2], Muhammad Ibadurrohman [1] and Mohammad Nasikin [1,*]

[1] Department of Chemical Engineering, Faculty of Engineering, Universitas Indonesia, Depok 16424, Indonesia; nadia.mumtazah@ui.ac.id (N.M.); ibad@che.ui.ac.id (M.I.)
[2] Research Center for Testing Technology and Standards, National Research and Innovation Agency, PUSPIPTEK Area, Tangerang Selatan 15314, Indonesia; nurf004@brin.go.id
* Correspondence: mnasikin@che.ui.ac.id
† Presented at the 4th Coatings and Interfaces Online Conference, 21–23 May 2025; Available online: https://sciforum.net/event/CIC2025.

Abstract

2,5-diformylfuran (DFF) is a significant biomass derivative that is employed in a variety of industries. One approach to synthesizing it is through the oxidation of 5-hydroxymethylfurfural (HMF). The challenges in DFF production arise from the need for extreme conditions, issues with overoxidation, and the limitations of noble materials used in neutral or acidic environments. By using a mildly alkaline electrolyte, DFF can be produced electrochemically alongside hydrogen gas generation, eliminating extreme conditions and allowing for the study of a wide range of transition metals. Moreover, the performance of bimetallic electrocatalysts has been studied, and it has been found to be more active in many kinds of processes, particularly Layered Double Hydroxides (LDH). Electrodeposition, once widely chosen among various LDH production methods, is preferred for producing controlled and uniform thin layers. This work examines the electrocatalytic properties of NiCo-LDH and NiFe-LDH in the production of DFF. Cobalt, which exhibits strong adsorption, will be compared to iron, which has a weak adsorption characteristic toward HMF. This study demonstrates that NiCo-LDH gives 1.49 V vs. RHE onset potential, 600 mV lower compared to NiFe-LDH (1.55 V vs. RHE) for HMF oxidation reaction. NiCo-LDH also converts twice the amount of HMF compared to NiFe-LDH for the same amount of charge passed at 0.25 mA/cm^{-2} in 0.1 M $Na_2B_4O_7$. However, strong adsorption promotes reactant activation and reduces the energy barrier while reducing DFF selectivity in NiCo-LDH (23.4%) due to overoxidation, compared to NiFe-LDH (31.6%). In order to achieve optimal electrocatalyst performance, a careful balance of adsorption strength and reaction pathway management is required. Proper optimization of these parameters is essential to improve efficiency and selectivity in the electrocatalytic process.

Keywords: 2,5-diformylfuran; 5-hydroxymethylfurfural; adsorption strength; layered double hydroxides; electrodeposition

check for updates

Academic Editor: Emerson Coy

Published: 10 November 2025

Citation: Mumtazah, N.; Syahlani, N.; Ibadurrohman, M.; Nasikin, M. Electrodeposition of Nickel-Based Thin Layered Double Hydroxides Electrocatalyst for 2,5-Diformylfuran Production. *Eng. Proc.* **2025**, *105*, 9. https://doi.org/10.3390/engproc2025105009

Copyright: © 2025 by the authors. Licensee MDPI, Basel, Switzerland. This article is an open access article distributed under the terms and conditions of the Creative Commons Attribution (CC BY) license (https://creativecommons.org/licenses/by/4.0/).

1. Introduction

2-Diformylfuran, often known as DFF, is a platform that is utilized extensively for the production of intermediates in polyethylene, diamines, antifungal compounds, and pharmaceuticals [1–4]. DFF can be produced through the oxidation of 5-hydroxymethylfurfural (HMF), a biomass derived compound. However, the investigation of HMF oxidation remains focused on generating 2,5-furandicarboxylic acid (FDCA) as the primary product in

the HMF oxidation reaction [5,6]. On the other hand, DFF is more challenging to obtain as an intermediate oxidation product than FDCA as a final product. Therefore, developing an effective catalyst for DFF production is necessary. The development of a catalyst for HMF oxidation has been reported in an oxygenated system demanding high-pressure gas or elevated temperatures [7–10]. The electrochemical oxidation method, on the other hand, is preferred because of its ease of control over the reaction route and selectivity [11], while depriving the needs of extreme circumstances [12] and providing hydrogen gas. Electrochemical oxidation of small molecules, such as HMF, has become a promising method for producing hydrogen efficiently, as it can take the place of the traditional oxygen evolution reaction in water electrolysis. For instance, selectively oxidation molecules from biomass or other small organics allows for the simultaneous production of hydrogen and value-added products under mild conditions. This lowers energy use and makes the whole process more efficient [13,14].

Noble metals such as platinum [15–18] and ruthenium [16,19] remain the dominant materials in electrocatalysis research for the oxidation of HMF to DFF. Raising temperature and pressure can achieve great selectivity when using noble metals. Acidic circumstances, which tend to limit the oxidation reaction, cause oxidation to occur. To avoid the utilization of severe temperatures and pressures, mild alkaline solutions have been used in the electrolysis of HMF into DFF. The application of this mild alkaline has resulted in an increase in research on electrocatalysts, including transition metal elements [20,21]. Transition metal electrocatalysts can be manufactured using a variety of methods, with electrodeposition being the most controlled for producing thin-layer electrocatalysts.

Electrodeposited electrocatalysis for HMF oxidation was investigated in nickel, iron, and cobalt-based materials [22–27], either as single or double metals. The performance of bimetallic electrocatalysts has been studied, and it has been found to be more active in many kinds of processes, particularly Layered Double Hydroxides (LDH) [28,29]. Furthermore, the previous study claimed that adding hydrogen peroxide to the precursor for LDH electrodeposition enhanced its performance [30]. Therefore, this study will use a nickel-based system, with cobalt (−4.79 eV) as the strongest adsorptive material for HMF and iron as the weakest (−1.82 eV) [31], as electrocatalysts made by the electrodeposition method to create a thin layer of LDHs to observe the generation of DFF from the HMF oxidation reaction. Furthermore, this study will provide an overview about the critical role of adsorption strength in balancing selectivity and efficiency during the electrocatalytic oxidation of HMF to produce DFF.

2. Materials and Methods

2.1. Materials and Reagents

Chemicals utilized in this study include the following: 5-(hydroxymethyl)furfural (HMF) (>99%, Sigma-Aldrich, Merck KGaA, Darmstadt, Germany); 2,5-furandicarboxaldehyde (DFF,) (97%, Sigma-Aldrich, Buchs, Switzerland); 5-Hydroxymethyl-2-furancarboxylic acid (HMFCA) (>95%, Sigma-Aldrich, Oakville, ON, Canada); $Ni(NO_3)_2{\cdot}6H_2O$ (99%, Sigma-Aldrich, Gillingham, United Kingdom); $CoCl_2{\cdot}6H_2O$ (99%, Sigma-Aldrich, Merck, Darmstadt, Germany); $FeCl_2{\cdot}4H_2O$ (99%, Sigma-Aldrich, Merck KGaA, Darmstadt, Germany); $Na_2B_4O_7$ (98%, Sigma-Aldrich, Merck KGaA, Darmstadt, Germany); Hydrogen Peroxide (30%, Sigma-Aldrich, Merck KGaA, Darmstadt, Germany); Nickel Plate (Sains laboratory, Jakarta, Indonesia); Aquadest.

2.2. Synthesis and Characterization of NiCo-LDHs and NiFe-LDHs

NiCo-LDH was manufactured through the electrodeposition method. First, a 50 mL solution containing 0.03 M $Ni(NO_3)_2.6H_2O$ and 0.015 M $CoCl_2.6H_2O$ was prepared. The

solution was subsequently mixed with 100 µL of 30% H_2O_2. This solution was used as an electrolyte for NiCo-LDHs electrodeposition on a prepared and cleaned nickel plate substrate (the area was maintained at 1 × 1 cm on both sides). The nickel plate was directly used as a working electrode. While Ag/AgCl in 3 M KCl and platinum mesh were used as reference and counter electrodes, respectively. Electrodeposition was carried out for 60 s at −1.0 V vs. Ag/AgCl [32–34] by potentiostat (Palmsens4). The mechanism describes in the following equations [28].

$$NO_3^- + H_2O + 2e^- \rightarrow NO_2^- + 2OH^- \quad (1)$$

$$M^{2+} + 2OH^- \rightarrow M(OH)_2 \quad (2)$$

Moreover, NiFe-LDH is made in a similar way as NiCo-LDH, with the exception of the use of $FeCl_2.4H_2O$ solution. For the Ni-Fe precursor, the solution was rested for 15 min to separate the undiluted precursor. The presence of layered double hydroxide was identified by X-ray powder diffraction (D8 Advance (Bruker, AXS GmbH, Karlsruhe, Germany), Bragg–Bentano Diffraction) at θ = 0.4 and FTIR (Thermo Scientific, Thermo Fisher Scientific, Waltham, MA, USA (Nicolet IS5), id7 atr transmission).

2.3. Electrochemical Measurement

Electrochemical HMF oxidation measurement was conducted by potentiostat (Palmsens4, PalmSens BV, Houten, The Netherlands). A three-electrode system was used in all experiments. The sample electrode was directly used as a working electrode. While Ag/AgCl in 3 M KCl and platinum mesh were used as reference and counter electrodes, respectively. All the potentials were converted to the reversible hydrogen electrode (RHE) as in the following equation.

$$E_{RHE} = E_{Ag/AgCl} + 0.059\ pH + 0.21 \quad (3)$$

The J-V or LSV curves of the electrocatalyst were performed at a scan rate of 10 mV/s. The electrochemical HMF oxidation was performed by chronopotentiometry in 50 mL $Na_2B_4O_7$ (pH 9.6) solution at room temperature and atmospheric pressure with stirring.

2.4. Product Analysis

All liquid products were analyzed by high-performance liquid chromatography (Nexera LC-40, Shimadzu Corporation, Kyoto, Japan) with a UV detector. The sample was separated by using the C18 column at 55 °C. The eluent was 5 mM sulfuric acid. The product of electrochemical HMF oxidation was detected by taking 200 µL of the electrolyte and diluting it with 1800 µL of pure water. The quantification of each electrolyte was determined based on the calibration curves obtained from the standard solution of known concentration. For the analysis, the DFF theoretical value was calculated based on the assumption that all passed charge is for DFF formation.

The *DFF selectivity (%)* was calculated using equations

$$DFF\ selectivity(\%) = \frac{DFF\ produced(mole)}{initial\ HMF(mole) - remaining\ HMF(mole)} \times 100\% \quad (4)$$

The *DFF faradaic efficiency (%)* was calculated using equations

$$DFF\ faradaic\ efficiency(\%) = \frac{DFF\ produced(mole)}{DFF\ theoritical(mole)} \times 100\% \quad (5)$$

3. Result and Discussion

3.1. Material Characterization

The SEM analysis (Figure 1) demonstrates that both NiCo-LDH and NiFe-LDH exhibits a homogeneous morphology with uniformly distributed particles in the nanoscale range, indicating that the resulting catalyst is nanostructured. The distribution of nanoparticles also shows the absence of agglomeration. In order to complement the morphological observations, the elemental composition of the samples was further examined using EDX analysis, and the corresponding spectra and quantitative results are provided in Table S1.

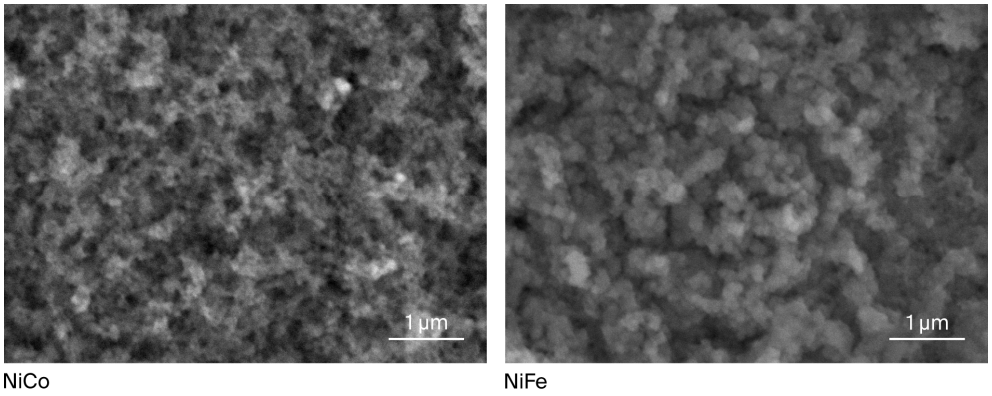


Figure 1. SEM image of the synthesized NiCo-LDH and NiFe-LDH electrocatalyst.

XRD has been employed to identify the basal spacing in LDH, which frequently appears at a low angle. In Figure 2a, NiFe-LDH reveals LDH peaks at 14.320° and 25.741°, which contribute to (003) and (006) reflections, respectively. The XRD patterns of NiFe-LDHs are in line with systematic reflections of the reference NiFe LDH [35]. Furthermore, these peaks at 14.263° and 25.732° can be recognized in the NiCo-LDH sample, showing that LDH was generated. The other peaks at 44.7°, 52.0°, and 76.6° correspond to the nickel plates used as substrates for the (111), (200), and (220) planes, respectively [36]. Additionally, these peaks also represent the arrangement of metal cations such as nickel, cobalt, and iron in the brucite-like structures. The intensity of these peaks varies depending on the atomic scattering factors of the cobalt and iron elements in the crystal lattice.

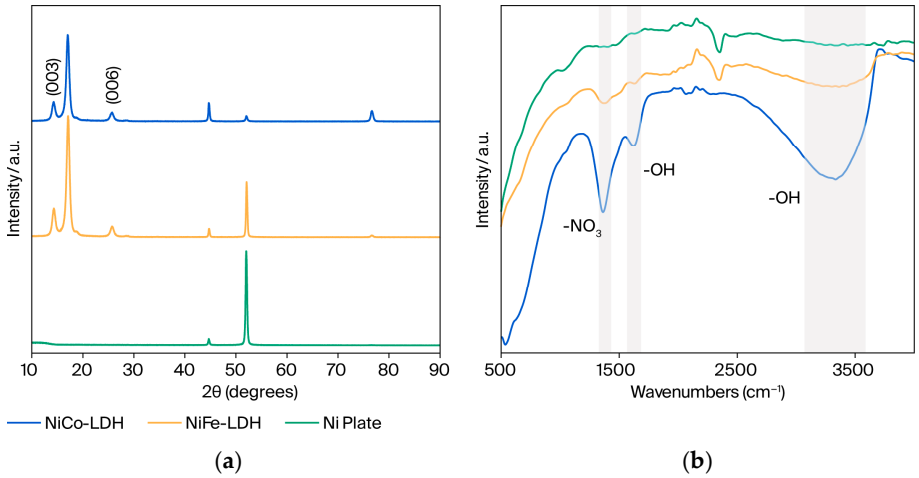


Figure 2. (**a**) XRD pattern and (**b**) FTIR spectra of prepared NiCo-LDH and NiFe-LDH.

LDH is known for its interlayered anions, such as carbonate ions, chloride ions, and nitrate ions, as well as neutral molecules, such as water molecules [37]. FTIR spectroscopy was used to identify LDH by establishing the presence of OH^- bonds and NO_3^- bonds

in the samples (Figure 2b). The broadening peak at 3200–3550 cm^{-1} contributes to the stretching mode of the OH^- group involving hydrogen bonding and interlayer molecules of water, which is similar to previously described substances [35]. Likewise, the band at ~1620 cm^{-1} corresponds to the bending mode of water. Furthermore, the ~1365 cm^{-1} contributes to the NO_3^- peak, revealing the LDH structure. However, the peak area of NiCo LDH is larger than NiFe LDH (Table S2) with the ratios 1:1.3, 1:1.2, and 1:1.4 for O-H stretching, O-H bending, and N-O stretching, respectively. Additionally, there is no apparent peak at such wavelengths in the bare nickel plate that is used as a substrate.

3.2. Electrochemical Characterization

DFF has high selectivity in medium alkaline circumstances or at lower pH values [6], whereas most metal transition materials suffer in neutral and acidic environments. In this study, pH 9.6 was chosen as a mild alkaline condition for DFF production by HMF oxidation. Figure 3a demonstrates the linear sweep voltammetry (LSV) curves of prepared NiCo-LDH and NiFe-LDH with and without HMF in the electrolyte. The onset potential of the oxygen evolution reaction (OER) is 1.52 V and 1.57 V vs. RHE for NiCo-LDH and NiFe-LDH, respectively. This value is approximately 200 mV higher than the onset potential of the HMF oxidation for each LDH sample. It implies that NiCo-LDH and NiFe-LDH electrocatalysts prefer to oxidize HMF over OER. The LSV curve of the bare nickel plate as a substrate for OER was also observed. Additionally, the influence of hydrogen peroxide in the precursor during electrodeposition was presented in Figure S1.

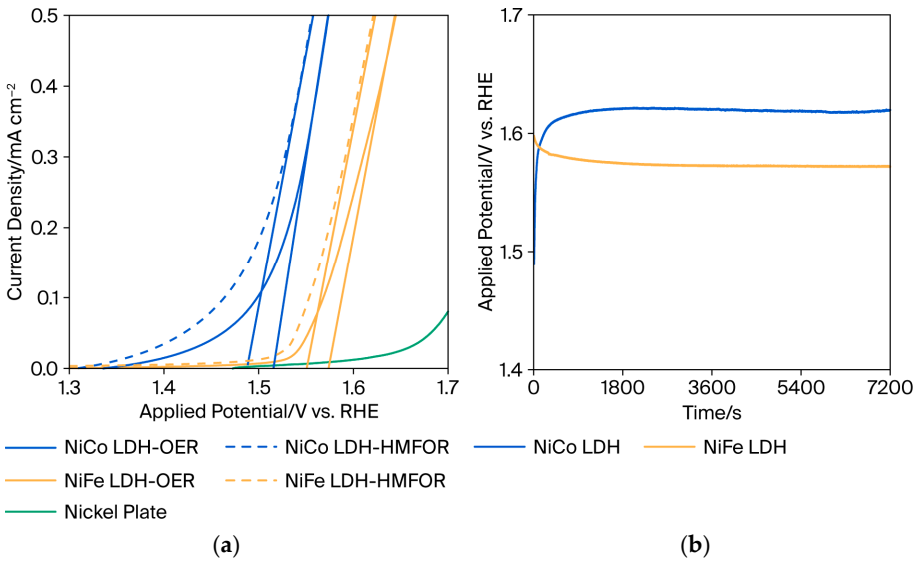


Figure 3. (**a**) Linear sweep voltammetry without (solid line) and with (dashed line) 20 mM HMF and (**b**) Chronopotentiometry of HMF oxidation at 0.25 mA/cm^{-2} in 0.1 M $Na_2B_4O_7$, 5 mM of HMF of prepared NiCo-LDH and NiFe-LDH.

Furthermore, Figure 3b shows a curve acquired during the chronopotentiometry test for HMF oxidation. Before both samples reached stable conditions, NiCo-LDH's applied potential increased with increasing reaction time. While at NiFe-LDH, the converse occurred. To achieve 0.25 mA/cm^{-2}, the NiCo-LDH needs 1.65 V vs. RHE after 2 h of reaction, while NiFe-LDH is stable at 1.57 V vs. RHE. The increase in applied potential implies that the reaction becomes less kinetically favorable with time. This could be because cobalt exhibits stronger adsorptive characteristics [31], which may initially increase activity but eventually lead to surface passivation or the accumulation of chemical intermediates. As the surface gets partially obstructed, the applied potential needs to rise to sustain the current. Iron materials, on the other hand, possess fewer adsorption features that could

potentially prevent surface passivation. Instead, the reaction intermediates are more easily desorbed, allowing the catalyst to perform more efficiently over time, resulting in a decrease in applied potential.

3.3. DFF Product Analysis

The oxidation of HMF is known to occur selectively at low applied potentials or currents. After oxidation, the product analysis results are summarized in Table 1. Based on obtained chromatogram data (Figure S2). During the reaction, the total charge transferred was 3.6 Coulombs. Despite using the same total charge for both samples, the HMF conversion for NiCo-LDH is about twice that of NiFe-LDH, indicating a higher activity. This difference indicates that a higher HMF oxidation reaction rate occurs in sample NiCo-LDH compared to NiFe-LDH. However, the low HMF conversion in sample NiFe-LDH suggests that the majority of the applied charge is not being effectively utilized for HMF oxidation. Instead, this charge might be consumed in competing reactions, such as the oxygen evolution reaction (OER) or other side reactions, or lost through non-Faradaic pathways like capacitive charging. In contrast, sample NiCo-LDH demonstrates a better balance between reaction rate and charge utilization.

Table 1. Oxidation of HMF using prepared NiCo-LDH and NiFe-LDH CuO for 2 h oxidation reaction time at 0.25 mA/cm^{-2} in 0.1 M $Na_2B_4O_7$ and 5 mM of HMF.

Sample	DFF Selectivity	DFF Faradaic Efficiency
NiCo-LDH	23.4%	42.6%
NiFe-LDH	31.6%	21.2%

Furthermore, the selectivity of DFF is higher in sample NiFe-LDH (31.6%) compared to sample NiCo-LDH (23.4%). This difference can be attributed to the adsorption strength of the catalysts. Fe is known to have weaker adsorption strength compared to Co [31] and binds intermediates only moderately, enabling a more selective conversion of HMF to DFF. In contrast, the stronger adsorption strength in sample NiCo-LDH can hinder the desorption of intermediate products, such as DFF, from the electrocatalyst surface. This prolonged interaction increases the likelihood of overoxidation, leading to the formation of by-products such as 5-Hydroxymethyl-2-furancarboxylic acid (HMFCA), 5-formyl-2-furoic acid (FFCA), or 2,5-furandicarboxylic acid (FDCA). Compared to NiCo-LDH, The NiFe-LDH might preferentially bind intermediates or reactants in a way that selectively favors the formation of DFF. However, inefficient charge transfer at the electrode-electrolyte interface or poor conductivity could limit the effective use of electrons, lowering Faradaic efficiency, as the DFF Faradaic Efficiency is 42.6% and 21.2% for NiCo-LDH and NiFe-LDH, respectively.

4. Conclusions

Electrodeposition of nickel-based layered double hydroxides (NiCo-LDH and NiFe-LDH) was employed for the electrocatalytic oxidation of HMF to DFF in a moderately alkaline electrolyte. NiCo-LDH and NiFe-LDH exhibited onset potentials of 1.50 V and 1.55 V vs. RHE, respectively, with the earlier onset potential of NiCo-LDH attributed to stronger HMF adsorption. After 2 h of reaction, NiCo-LDH required 1.65 V vs. RHE to reach 0.25 mA cm^{-2}, whereas NiFe-LDH required 1.57 V vs. RHE, indicating a greater kinetic hindrance over time for NiCo-LDH. The stronger adsorption of HMF on NiCo-LDH led to higher HMF conversion and Faradaic efficiency but lower DFF selectivity, likely due to desorption limitations and overoxidation. These results demonstrate that adsorption strength

plays a decisive role in balancing selectivity and efficiency during HMF oxidation and that tuning adsorption properties is essential for enhancing electrocatalytic performance.

Supplementary Materials: The following supporting information can be downloaded at: https://www.mdpi.com/article/10.3390/engproc2025105009/s1, Figure S1. Linear sweep voltammetry of NiCo-LDH and NiFe-LDH with (solid line) and without (dashed line) hydrogen peroxide in the precursor during electrodeposition. Figure S2. Chromatogram data obtained from HPLC after HMF oxidation reaction in 2 h using NiCo-LDH and NiFe-LDH. Table S1. EDX elemental composition of the synthesized electrocatalyst, showing the relative mass and atomic percentages of the constituent elements. Table S2. Peak Area Comparison of NiCo LDH and NiFe-LDH.

Author Contributions: Conceptualization, N.M., M.I. and M.N.; methodology, N.M.; software, N.M.; validation, M.I. and M.N.; formal analysis, N.M. and M.I.; investigation, M.I. and M.N.; resources, N.M. and N.S.; data curation, N.M., M.I., N.S. and M.N.; writing—original draft preparation, N.M.; writing—review and editing, M.I., N.S. and M.N.; visualization, N.M.; supervision, M.I. and M.N. All authors have read and agreed to the published version of the manuscript.

Funding: The authors disclosed receipt of the following financial support for the research, authorship, and/or publication of this article: This research was funded and supported by Doctoral's program scholarship of the Indonesian education scholarship, Lembaga Pengelola Dana Pendidikan (LPDP).

Institutional Review Board Statement: Not applicable.

Informed Consent Statement: Not applicable.

Data Availability Statement: The data used to support the finding of this study are included within the article.

Conflicts of Interest: The authors declare no conflicts of interest.

References

1. Chen, Z.; Liao, S.; Ge, L.; Amaniampong, P.N.; Min, Y.; Wang, C.; Li, K.; Lee, J.-M. Reduced graphene oxide with controllably intimate bifunctionality for the catalytic transformation of fructose into 2, 5-diformylfuran in biphasic solvent systems. *Chem. Eng. J.* **2020**, *379*, 122284. [CrossRef]
2. Qi, H.; Liu, F.; Zhang, L.; Li, L.; Su, Y.; Yang, J.; Hao, R.; Wang, A.; Zhang, T. Modulating trans-imination and hydrogenation towards the highly selective production of primary diamines from dialdehydes. *Green Chem.* **2020**, *22*, 6897–6901. [CrossRef]
3. Silbert, S.D.; Serum, E.M.; LaScala, J.; Sibi, M.P.; Webster, D.C. Biobased, nonisocyanate, 2K polyurethane coatings produced from polycarbamate and dialdehyde cross-linking. *ACS Sustain. Chem. Eng.* **2019**, *7*, 19621–19630. [CrossRef]
4. Zhao, D.; Su, T.; Wang, Y.; Varma, R.S.; Len, C. Recent advances in catalytic oxidation of 5-hydroxymethylfurfural. *Mol. Catal.* **2020**, *495*, 111133. [CrossRef]
5. Gidi, L.; Amalraj, J.; Tenreiro, C.; Ramirez, G. Recent progress, trends, and new challenges in the electrochemical production of green hydrogen coupled to selective electrooxidation of 5-hydroxymethylfurfural (HMF). *RSC Adv.* **2023**, *13*, 28307–28336. [CrossRef]
6. Guo, L.; Zhang, X.; Gan, L.; Pan, L.; Shi, C.; Huang, Z.F.; Zhang, X.; Zou, J.J. Advances in Selective Electrochemical Oxidation of 5-Hydroxymethylfurfural to Produce High-Value Chemicals. *Adv. Sci.* **2023**, *10*, e2205540. [CrossRef]
7. Wan, Y.; Lee, J.-M. Toward value-added dicarboxylic acids from biomass derivatives via thermocatalytic conversion. *ACS Catal.* **2021**, *11*, 2524–2560. [CrossRef]
8. Zhao, J.; Chen, X.; Du, Y.; Yang, Y.; Lee, J.-M. Vanadium-embedded mesoporous carbon microspheres as effective catalysts for selective aerobic oxidation of 5-hydroxymethyl-2-furfural into 2, 5-diformylfuran. *Appl. Catal. A Gen.* **2018**, *568*, 16–22. [CrossRef]
9. Zhou, W.; Kong, Z.; Wu, Z.; Yang, S.; Wang, Y.; Liu, Y. Efficient oxidation of biomass derived 5-hydroxymethylfurfural into 2,5-diformylfuran catalyzed by NiMn layered double hydroxide. *Catal. Commun.* **2021**, *151*, 106279. [CrossRef]
10. Neaţu, F.; Petrea, N.; Petre, R.; Somoghi, V.; Florea, M.; Parvulescu, V.I. Oxidation of 5-hydroxymethyl furfural to 2,5-diformylfuran in aqueous media over heterogeneous manganese based catalysts. *Catal. Today* **2016**, *278*, 66–73. [CrossRef]
11. Simoska, O.; Rhodes, Z.; Weliwatte, S.; Cabrera-Pardo, J.R.; Gaffney, E.M.; Lim, K.; Minteer, S.D. Advances in Electrochemical Modification Strategies of 5-Hydroxymethylfurfural. *ChemSusChem* **2021**, *14*, 1674–1686. [CrossRef] [PubMed]
12. Kwon, Y.; Schouten, K.J.P.; van der Waal, J.C.; de Jong, E.; Koper, M.T.M. Electrocatalytic Conversion of Furanic Compounds. *ACS Catal.* **2016**, *6*, 6704–6717. [CrossRef]

13. Sun, H.; Xu, X.; Fei, L.; Zhou, W.; Shao, Z. Electrochemical Oxidation of Small Molecules for Energy-Saving Hydrogen Production. *Adv. Energy Mater.* **2024**, *14*, 2401242. [CrossRef]
14. Du, L.; Sun, Y.; You, B. Hybrid water electrolysis: Replacing oxygen evolution reaction for energy-efficient hydrogen production and beyond. *Mater. Rep. Energy* **2021**, *1*, 100004. [CrossRef]
15. Vuyyuru, K.R.; Strasser, P. Oxidation of biomass derived 5-hydroxymethylfurfural using heterogeneous and electrochemical catalysis. *Catal. Today* **2012**, *195*, 144–154. [CrossRef]
16. Cao, T.; Wu, M.; Ordomsky, V.V.; Xin, X.; Wang, H.; Métivier, P.; Pera-Titus, M. Selective Electrogenerative Oxidation of 5-Hydroxymethylfurfural to 2,5-Furandialdehyde. *ChemSusChem* **2017**, *10*, 4851–4854. [CrossRef]
17. Kubota, S.R.; Choi, K.S. Electrochemical Oxidation of 5-Hydroxymethylfurfural to 2,5-Furandicarboxylic Acid (FDCA) in Acidic Media Enabling Spontaneous FDCA Separation. *ChemSusChem* **2018**, *11*, 2138–2145. [CrossRef]
18. Latsuzbaia, R.; Bisselink, R.; Anastasopol, A.; van der Meer, H.; van Heck, R.; Yagüe, M.S.; Zijlstra, M.; Roelands, M.; Crockatt, M.; Goetheer, E.; et al. Continuous electrochemical oxidation of biomass derived 5-(hydroxymethyl)furfural into 2,5-furandicarboxylic acid. *J. Appl. Electrochem.* **2018**, *48*, 611–626. [CrossRef]
19. Ge, R.; Wang, Y.; Li, Z.; Xu, M.; Xu, S.-M.; Zhou, H.; Ji, K.; Chen, F.; Zhou, J.; Duan, H. Selective Electrooxidation of Biomass-Derived Alcohols to Aldehydes in a Neutral Medium: Promoted Water Dissociation over a Nickel-Oxide-Supported Ruthenium Single-Atom Catalyst. *Angew. Chem. Int. Ed.* **2022**, *61*, e202200211. [CrossRef] [PubMed]
20. Le, T.-H.-H.; Vo, T.-G.; Chiang, C.-Y. Highly efficient amorphous binary cobalt-cerium metal oxides for selective oxidation of 5-hydroxymethylfurfural to 2,5-diformylfuran. *J. Catal.* **2021**, *404*, 560–569. [CrossRef]
21. Mumtazah, N.; Chan, C.-H.; Catherine, S.; Pham, M.-T.H.; Choi, J.; Yoo, J.S.; Chiang, C.-Y. Modulating surface chemistry of copper oxides through annealing environment for enhanced selective HMF oxidation: A DFT-electrochemical approach. *J. Environ. Chem. Eng.* **2024**, *12*, 113444. [CrossRef]
22. Nam, D.H.; Taitt, B.J.; Choi, K.S. Copper-Based Catalytic Anodes to Produce 2,5-Furandicarboxylic Acid, a Biomass-Derived Alternative to Terephthalic Acid. *ACS Catal.* **2018**, *8*, 1197–1206. [CrossRef]
23. Zhong, Y.; Ren, R.Q.; Qin, L.; Wang, J.B.; Peng, Y.Y.; Li, Q.; Fan, Y.M. Electrodeposition of hybrid nanosheet-structured NiCo2O4on carbon fiber paper as a non-noble electrocatalyst for efficient electrooxidation of 5-hydroxymethylfurfural to 2,5-furandicarboxylic acid. *New J. Chem.* **2021**, *45*, 11213–11221. [CrossRef]
24. Zhu, B.; Chen, C.; Huai, L.; Zhou, Z.; Wang, L.; Zhang, J. 2,5-Bis(hydroxymethyl)furan: A new alternative to HMF for simultaneously electrocatalytic production of FDCA and H2 over CoOOH/Ni electrodes. *Appl. Catal. B Environ.* **2021**, *297*, 120396. [CrossRef]
25. Zhang, B.; Fu, H.; Mu, T. Hierarchical NiSx/Ni2P nanotube arrays with abundant interfaces for efficient electrocatalytic oxidation of 5-hydroxymethylfurfural. *Green Chem.* **2022**, *24*, 877–884. [CrossRef]
26. Xu, H.; Xin, G.; Hu, W.; Zhang, Z.; Si, C.; Chen, J.; Lu, L.; Peng, Y.; Li, X. Single-atoms Ru/NiFe layered double hydroxide electrocatalyst: Efficient for oxidation of selective oxidation of 5-hydroxymethylfurfural and oxygen evolution reaction. *Appl. Catal. B Environ.* **2023**, *339*, 123157. [CrossRef]
27. Carvajal, D.; Arcas, R.; Gouda, L.; Fabregat-Santiago, F.; Mas-Marzá, E. Electrochemical valorization of HMF using Ni/Graphite electrodes. *Mater. Chem. Phys.* **2024**, *311*, 128510. [CrossRef]
28. Rohit, R.C.; Jagadale, A.D.; Shinde, S.K.; Kim, D.Y. A review on electrodeposited layered double hydroxides for energy and environmental applications. *Mater. Today Commun.* **2021**, *27*, 102275. [CrossRef]
29. Ji, W.; He, Y.; Zhang, T.C.; Wang, Y.; Yuan, S. Nickel-based non-noble metal layered double hydroxide grown on carbon cloth for boosting electrocatalytic oxidation of As(III). *Appl. Surf. Sci.* **2023**, *618*, 156631. [CrossRef]
30. Tang, Y.; Shen, H.; Cheng, J.; Liang, Z.; Qu, C.; Tabassum, H.; Zou, R. Fabrication of Oxygen-Vacancy Abundant NiMn-Layered Double Hydroxides for Ultrahigh Capacity Supercapacitors. *Adv. Funct. Mater.* **2020**, *30*, 1908223. [CrossRef]
31. Yang, Y.; Xu, D.; Zhang, B.; Xue, Z.; Mu, T. Substrate molecule adsorption energy: An activity descriptor for electrochemical oxidation of 5-Hydroxymethylfurfural (HMF). *Chem. Eng. J.* **2022**, *433*, 133842. [CrossRef]
32. Yoon, S.; Yun, J.-Y.; Lim, J.-H.; Yoo, B. Enhanced electrocatalytic properties of electrodeposited amorphous cobalt-nickel hydroxide nanosheets on nickel foam by the formation of nickel nanocones for the oxygen evolution reaction. *J. Alloys Compd.* **2017**, *693*, 964–969. [CrossRef]
33. Bo, X.; Li, Y.; Chen, X.; Zhao, C. High valence chromium regulated cobalt-iron-hydroxide for enhanced water oxidation. *J. Power Sources* **2018**, *402*, 381–387. [CrossRef]
34. Bo, X.; Li, Y.; Hocking, R.K.; Zhao, C. NiFeCr Hydroxide Holey Nanosheet as Advanced Electrocatalyst for Water Oxidation. *ACS Appl. Mater. Interfaces* **2017**, *9*, 41239–41245. [CrossRef]
35. Qu, J.; Li, F.; Wang, M.; Subakti, S.; Deconinck, M.; Chen, G.; Li, Y.; Liu, L.; Wang, X.; Yu, M.; et al. One-Pot Synthesis of Nitrate-Intercalated NiFe Layered Double Hydroxides with an 8.2 Å Interlayer Spacing. *Adv. Mater. Interfaces* **2022**, *9*, 2200973. [CrossRef]

36. Sassi, W.; Dhouibi, L.; Bercot, P.; Rezrazi, E.M.; Triki, E. Comparative study of protective nickel–tungsten deposit behavior obtained by continuous and pulsed currents from citrate–ammonia media. *Surf. Coat. Technol.* **2012**, *206*, 4235–4241. [CrossRef]
37. Stamate, A.-E.; Pavel, O.D.; Zavoianu, R.; Marcu, I.-C. Highlights on the Catalytic Properties of Polyoxometalate-Intercalated Layered Double Hydroxides: A Review. *Catalysts* **2020**, *10*, 57. [CrossRef]

Disclaimer/Publisher's Note: The statements, opinions and data contained in all publications are solely those of the individual author(s) and contributor(s) and not of MDPI and/or the editor(s). MDPI and/or the editor(s) disclaim responsibility for any injury to people or property resulting from any ideas, methods, instructions or products referred to in the content.